


Article

Removal of Thiophenol from Water Using Sepiolite

Katarzyna Chruszcz-Lipska 

Department of Oil Engineering, Faculty of Drilling, Oil and Gas, AGH University of Krakow, Mickiewicza 30 Ave., 30-059 Kraków, Poland; lipska@agh.edu.pl

Abstract: Crude oil and petroleum products contain various types of sulfur compounds: aliphatic and aromatic mercaptans, hydrogen sulfide, sulfides, disulfides, thiophene derivatives, etc. Some of these may dissolve in water only slightly, but their toxicity and corrosiveness indicate that even these small amounts should be eliminated from water. This work examines, for the first time, the removal of thiophenol (synonyms: benzenethiol, phenyl mercaptan) from water using sepiolite. This clay mineral (evaluated by SEM analysis) is an attractive natural sorbent characterized by its microporosity, which results from its crystalline structure and large specific surface area. Because the structure of thiophenol changes depending on the pH of the aqueous solution (due to the loss of a proton), the research was conducted at pH 4, 7 and 9. The detection of thiophenol in aqueous solution was investigated using UV spectroscopy. It was found that the adsorption of thiophenol is possible, but it occurs only in an acidic environment (pH 4). No sorption is observed at pH 7 or 9. The adsorption of thiophenol at pH 4 does not change significantly after changing the ionic strength of the aqueous solution (distilled water, 0.01 NaCl and 0.1 NaCl). The adsorption capacity of sepiolite is approximately 0.23–0.34 mg/g. Studies using infrared spectroscopy and fitting of Freundlich and Langmuir isotherm models to the results of adsorption experiments indicate that adsorption on unmodified sepiolite follows a physisorption mechanism. Additionally, to understand the behavior of thiophenol in the presence of sepiolite across different pH ranges, DFT/PCM/B3LYP/Aug-CC-pVDZ calculations were used to analyze the charge distribution on particular atoms in its structure.

Keywords: thiophenol; clay minerals; sepiolite; removal from water; positive and negative adsorption; UV spectroscopy



Citation: Chruszcz-Lipska, K.

Removal of Thiophenol from Water Using Sepiolite. *Minerals* **2024**, *14*, 743. <https://doi.org/10.3390/min14080743>

Academic Editors: Mario Nikola Mužek and Sandra Svilović

Received: 25 April 2024

Revised: 19 July 2024

Accepted: 22 July 2024

Published: 24 July 2024



Copyright: © 2024 by the author. Licensee MDPI, Basel, Switzerland. This article is an open access article distributed under the terms and conditions of the Creative Commons Attribution (CC BY) license (<https://creativecommons.org/licenses/by/4.0/>).

1. Introduction

Sulfur is the third most abundant element in crude oil: its content is usually in the range of 1%–4% by weight, but higher levels, up to 14%, are known [1–3]. Most of the sulfur is incorporated into the structures of various aliphatic, cycloaliphatic, aromatic, or heterocyclic organic compounds, which, due to their different properties, occur in almost all fractions during crude oil processing [1]. The presence of sulfur compounds in crude oil is undesirable as it causes corrosion problems during petroleum processing and transport (pipelines, pumping equipment and refinery installations) and also disruptions in the operation of catalysts used in the refining process [4,5]. Sulfur has a negative impact on the quality of petroleum products and may additionally cause environmental problems (for example, by polluting the air with sulfur dioxide resulting from fuel combustion). Therefore, the oil industry must work to provide the best desulfurization technologies for crude oil and petroleum products [4,6–8]. On the other hand, the modern economy needs supplies of isolated sulfur compound concentrates for the production of a range of products that are necessary in other industries and people's everyday lives, including pharmaceuticals, pesticides, detergents, dyes, plastics, and various other products [9–12].

Thiophenol (Figure 1) belongs to the family of volatile organic compounds and is introduced to the environment mainly through anthropogenic sources [13]. Thiophenol may be a component of petroleum [1], but it is, for example, also a monomer of polyphenylene

sulfide (PPS) [9]. PPS, as well as PPS mixtures and composites, are characterized by interesting properties, such as high mechanical, thermal and acid resistance. Therefore, they are widely used in various modern industries for the production of automotive and aerospace components, electronic materials, durable chemical containers, materials for dust filters and separation membranes, medical tools etc. [9–11].

Thiophenol is toxic to organisms; it can pollute water and due to its volatility, also the air [14].

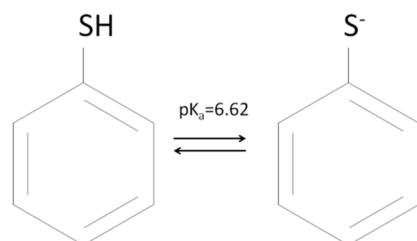


Figure 1. pH-dependent structure of thiophenol in aqueous solution, pKa according to [15].

Therefore, the search for reliable methods of detection and effective removal of thiophenol from the environment is very necessary. The latest research shows that it is possible to detect thiophenols quickly, and with high accuracy, in water as well as in food, soil, and plant samples [16–19]. In turn, there is a lack of studies showing methods of removal of thiophenol from the aquatic environment.

Recently, various materials, processes and technological solutions have been used to remove organic pollutants from water [20,21]. Adsorption technology is an extremely useful method due to its efficiency, simplicity, low cost, low energy consumption and environmental friendliness [22]. In turn, clay minerals are cheap, non-toxic green materials that are easily available in nature and can be successfully used as an adsorbent in water purification systems [23]. Moreover, clay minerals (mainly smectite, illite, chlorite and kaolinite) are natural components of marine sediments [24]. In addition, clay minerals enable good development of bacteria that decompose hydrocarbons, which may be important for the self-purification of seawater from petroleum hydrocarbons [25].

This work presents the possibility of adsorption of thiophenol on sepiolite, which is a magnesium silicate with a layer-ribbon structure [26]. Its chemical formula is $Mg_4Si_6O_{15}(OH)_2 \cdot 6H_2O$ [27]. Sepiolite crystallizes in the orthorhombic system. The parameters of the unit cell determined for different samples of sepiolite are similar: $a = 13.4 \text{ \AA}$, $b = 26.8 \text{ \AA}$, $c = 5.28 \text{ \AA}$ [28]; $a = 13.50 \text{ \AA}$, $b = 26.97 \text{ \AA}$, $c = 5.25 \text{ \AA}$ [29]; $a = 13.405 \text{ \AA}$, $b = 27.016 \text{ \AA}$, $c = 5.275 \text{ \AA}$ [30], and $a = 13.395 \text{ \AA}$, $b = 27.016 \text{ \AA}$, $c = 5.277 \text{ \AA}$ [31]. Sepiolite may have a high specific surface area (SSA) above $300 \text{ m}^2/\text{g}$ due to its small particle size and specific porous crystal structure. According to Suarez and Garcia-Romero [32], who examined 22 samples of natural sepiolites, the specific surface area (BET—Brunauer-Emmett-Teller) was from 77 to $399 \text{ m}^2/\text{g}$. Nishimura et al. [33] and Shuali et al. [34] found that the BET surface area for sepiolite ranges between 80 and $350 \text{ m}^2/\text{g}$, and 230 and $320 \text{ m}^2/\text{g}$, respectively.

According to literature data, sepiolite in its natural and modified forms is widely used in sorption processes of various organic compounds [35–39]. It is known as a good adsorbent for removing various types of aromatic organic compounds found in the gaseous [40] and liquid phases [41], or dissolved in water [35–39]. Sepiolite can bind gaseous organic sulfur compounds, such as mercaptans or cyclic sulfides, including thiophene and thiophenol [40]. Sepiolite has been shown to be an effective adsorbent in the adsorption of surface oil spills (edible and hydraulic oil) [41]. It can also be used in water purification cartridges and as a bottom liner material in solid waste landfills for the retention of organic and inorganic pollutants [42–44].

The available literature data shows that this work is the first to present research on the removal of toxic thiophenol from water using sorption processes. Since the structure of thiophenol is pH-dependent (Figure 1), the research was conducted in alkaline, acidic, and

neutral environments. As a sorbent in this work, we used sepiolite, which belongs to the family of clay minerals, which are considered cheap, chemically and mechanically stable, and efficient porous sorbents for organic pollutants [41,45,46]. Sepiolite is characterized by natural microporosity resulting from its crystalline structure and large specific surface, which is very attractive in the design of sorbents.

2. Materials and Methods

2.1. Materials

Liquid thiophenol, declared purity 99%, was purchased from Aldrich (Sigma-Aldrich Chemie GmbH, Schnelldorf, Germany) and used as obtained without further purification. Sepiolite ($\text{Mg}_2\text{H}_2\text{Si}_3\text{O}_9 \cdot x\text{H}_2\text{O}$) (powder, ~13% Mg, $\leq 10\%$ loss on drying, quality level 100, $d = 2.0\text{--}2.3 \text{ g/cm}^3$) was purchased from Sigma-Aldrich (Schnelldorf, Germany) and used unmodified.

2.2. SEM Photographs

The sepiolite sample was investigated using an FEI QUANTA FEG 200 scanning electron microscope (SEM) (Thermo Fisher Scientific, Waltham, MA, USA). This sample was imaged under a low vacuum with no conductive coating applied.

2.3. UV Spectroscopy

The ultraviolet (UV) spectra were recorded using a UV-Vis spectrometer (Shimadzu UV-1700) (Shimadzu Cooperation, Kyoto, Japan) in the range of 190–400 nm with an accuracy of 1 nm. The instrument was connected to a computer and operated by the UV Probe program. The measurements were performed for samples which were aqueous solutions. The spectrometer used was a double-beam spectrometer; therefore, pure distilled water was used as a reference sample.

UV spectra measurements for a solution of pure thiophenol in distilled water were performed in the pH range 4–12; the pH was changed by adding 0.1 M NaOH solution or 0.1 M HCl. Measurements of the content of thiophenol in aqueous solution in the adsorption process were made after double centrifugation of the sepiolite.

2.4. IR Spectroscopy

Fourier transform infrared (FT-IR) spectra of the samples were recorded using an Avatar 360 FT-IR spectrometer (Thermo Nicolet, Thermo Fisher Scientific, Waltham, MA, USA). The KBr pellet method with transmission mode was used. The spectra were collected at room temperature in the mid-infrared spectral range ($3800\text{--}400 \text{ cm}^{-1}$) with 256 scans at a spectral resolution of 2 cm^{-1} . Some of the infrared spectra in this work were additionally measured using the attenuated total reflectance Fourier transform infrared (ATR-FTIR) technique using a Bruker VERTEX 70v FT-IR spectrometer (Bruker, Ettlingen, Germany). The spectra were recorded in the spectral range of $2000\text{--}400 \text{ cm}^{-1}$, and 32 scans were averaged at a resolution of 2 cm^{-1} .

2.5. DFT Calculations of Atomic Charge

Atomic charge, defined as the distribution of charge within a molecule, is an important property of a molecule. Atomic charge is related to the structure of a chemical compound and implies the formation of interactions between other molecules in its surroundings, as well as between its individual fragments (especially for large complex structures) [47]. Consequently, the distribution of atomic charge in a molecule is also responsible for its chemical reactivity. Atomic charge is not a quantum mechanical observable [48]. Theoretical methods using computational chemistry are one way of determining the atomic charge of a molecule. In this work, values of atomic charges in molecules were calculated by population analysis determined using Cioslowski's APT (Atomic Polar Tensor), based on the trace of the dipole moment derivatives [49]. APT gives reasonable quantitative results and allows the interpretation of intramolecular chemical/physical effects occurring within

and between molecules [50]. Calculations were conducted using the Gaussian'16 package of programs [51]. Different forms of thiophenol as single molecules were studied at the density functional theory (DFT) level using the B3LYP functional and the Aug-CC-pVDZ basis set [52–54]. To best reflect the experimental conditions, the geometry optimization, the IR spectrum and the charge distribution in the molecule were calculated using the solvation model (PCM—Polarizable Continuum Model) implemented in Gaussian'16 [51]. The use of a computational solvation model allows for a better description of the behavior of the molecules in an appropriate solution (in our case, aqueous). In the PCM method, the solvent model is implemented in such a way that the solute occupies a cavity with a solvent field characterized by its individual dielectric constant [48].

2.6. Experimental Studies of the Adsorption Process

Experiments examining the influence of the thiophenol contact time with the sepiolite during the sorption process were carried out according to the scheme shown in Figure 2. Because the form of thiophenol depended on the pH of the solution (dissociated and undissociated, Figure 1), the process was carried out at pH regimes 4, 7 and 9. Each time, 100 mL of thiophenol solution (in distilled water) at a concentration of 5 mg/L and at an appropriate pH, was added to vessel with 1 g of sepiolite. After adding the adsorbate to the sepiolite, the sample was continuously stirred on a magnetic stirrer at a speed of 100 rpm. During this uninterrupted process, 1 mL samples were taken from the center of the vessel at various time intervals. After double centrifugation of sepiolite, these samples were investigated using UV spectroscopy. The process was conducted several times and only a few samples were taken each time to avoid significant errors related to disturbing the ratio of thiophenol to sepiolite in the solution. The pH of the solution was monitored and, if necessary, corrected during the whole duration of the process, which was conducted at room temperature.

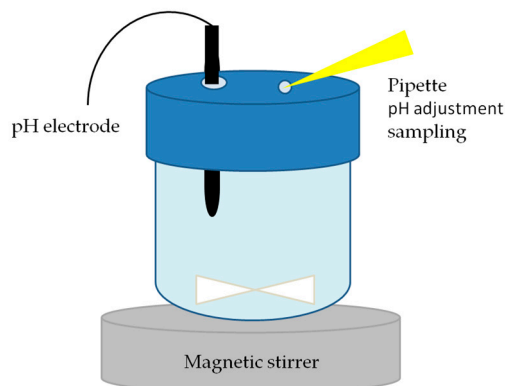


Figure 2. Scheme of an experiment examining the contact time in the sorption process.

The relationship between the amount of adsorbed substance and the concentration of this substance in the solution at the moment of adsorption equilibrium was also studied. Each time, 100 mL of thiophenol solution with a concentration of 5 mg/L and an appropriate pH were added to vessel with 0.1, 0.2, 0.3, 0.4, 0.5, 0.6, 0.7, 0.8, 0.9, 1.0, 1.2, 1.5, 1.7, and 2.0 g of sepiolite. Then, the tightly closed vessels were shaken on an orbital shaker (120 rpm) for 2 h, left for another 2 h, then UV spectra were taken to measure the thiophenol concentration above the sediment of sepiolite.

At pH 4, the influence of the ionic strength of the thiophenol solution on the sorption kinetics and sorption isotherm was also examined. In this case, thiophenol was also dissolved in 0.01 M and 0.1 M NaCl solutions.

3. Results

3.1. Characteristics of Sepiolite

The morphology of sepiolite used for sorption studies was examined by SEM analysis. In Figure 3, fiber-shaped sepiolite crystals can be clearly observed, packed very loosely into the light porous material. The fibrous morphology of sepiolite results from the regular molecular organization of the crystals of this clay mineral [55]. The sepiolite was also characterized by IR spectroscopy (see Section 3.6).

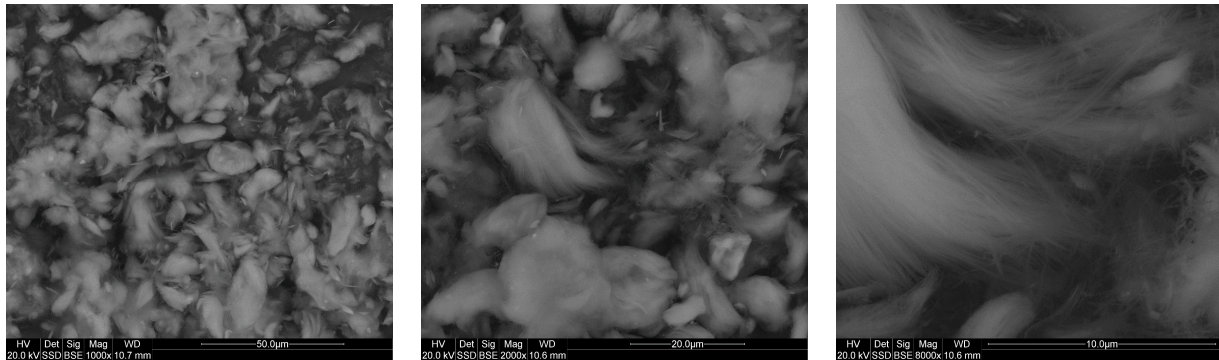


Figure 3. SEM micrographs of the sepiolite fibers at three different scales: 50, 20 and 10 μm .

3.2. Detection of Thiophenol in Aqueous Solution by UV Spectroscopy

UV spectroscopy is a known method for detection of chemical compounds containing the SH moiety, especially in refinery waste water [56,57]. In the UV spectra of inorganic sulfide, for a pH higher than 7, a band with a maximum at 231 nm is observed [56]. In alkaline solution, the predominant form of inorganic sulfides is the HS^- anion, and light from the UV region promotes the excitation of the unshared electrons, n , of the sulfur atom ($n \rightarrow \pi^*$). The UV spectra of aliphatic mercaptans (R-SH) like ethanethiol and propanethiol are also pH dependent. In acidic media, where the undissociated form of thiol predominates, no absorption bands are observed. In turn, in alkaline media these compounds in thiolate forms show absorption at a maximum of 238 nm. The UV spectra of thiophenols exhibit a greater number of spectral bands. A benzene ring of thiophenol is an element of the structure which affects the stabilization of the negative charge with π electrons of the aromatic ring. Figure 4 shows UV spectra of thiophenol at different pH values in the 190–350 nm range. These spectra are similar to those previously presented by Roig et al. [57]. In alkaline media, the thiolate ion shows absorption at 202 and 263 nm. In acidic media, the UV spectrum of thiophenol reveals bands at 202 and 236 nm. Figure 4 shows that the two absorption bands, at maximums of 236 and 263 nm, are clearly associated with the undissociated and dissociated forms of thiophenol, respectively. It can also be observed that the pKa value ($\text{pK}_a = 6.62$, Figure 1) is certainly in the range of pH 6–7, because in this range one of the bands disappears and the other appears.

In order to correctly determine the exact concentration of thiophenol in a solution, apart from determining the appropriate pH, the stability of the solutions is also important. Roig et al. [57] point out that a 40 mg/L solution of ethanethiol at pH 11 maintains a given concentration for approximately 15 min. In the presence of dissolved oxygen, especially at high pH values, oxidation of the compound occurs. Moreover, thiophenol is a volatile substance and any activities related to sampling the solution may affect the final concentration. Figure 5 shows the evolution of the absorbance of the thiophenol solutions (5 mg/L) with time.

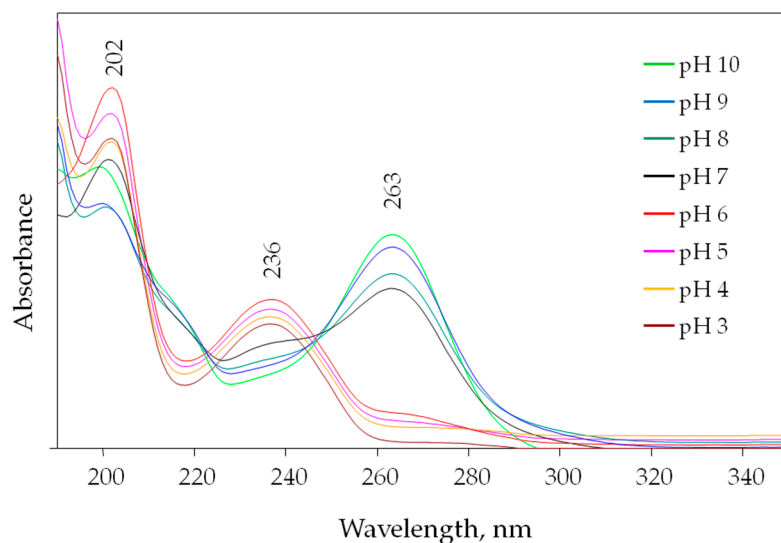


Figure 4. Evolution of UV spectra for an aqueous solution of thiophenol (5 mg/L) with pH.

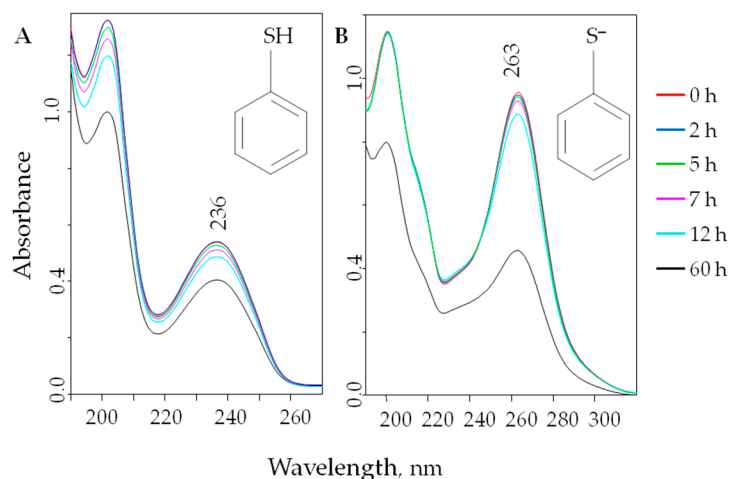


Figure 5. Evolution of absorbance of the thiophenol solutions with time (in hours): (A) concentration 5 mg/L, pH 3.5 (thiol); (B) concentration 5 mg/L, pH 9.0 (thiolate).

The 5 mg/L solutions of thiophenol are stable for 2 h, and the concentration is very close to 100%. After 5 h, 98.5%–99.0% of the initial concentration remains. Therefore, absorbance measurements of the solution used to prepare the calibration curve were performed immediately after their preparation and all sorption tests were performed using freshly prepared solutions. To determine the concentration of thiophenol in a solution, two different calibration curves for two different pH values (pH 4 and pH 9) were created by measuring the absorbance (at 236 and 263 nm, respectively) of the standard solutions (1.0, 2.0, 3.0, 4.0, 5.0 mg/L). A good correlation was obtained between the concentration of thiophenol in distilled water and the absorbance at both 236 nm (thiophenol, pH 4) and 263 nm (thiophenol in the form of thiophenolate, pH 9). The linear regression parameter was $R^2 = 0.9894$ and 0.9970 for absorption at 236 and 263 nm, respectively. The linear regression fitting data indicate that UV spectroscopy is well suited to measuring thiophenol concentrations in aqueous solutions.

3.3. The Influence of pH, Ionic Strength and Contact Time on the Adsorption Process of Thiophenol on Sepiolite

As previously shown, thiophenol in a water solution can occur in neutral and anionic forms (Figure 1). The surface of clay minerals is negative; in addition, increasing the

pH of the solution increases this negative charge [58]. For this reason, the adsorption of anions on clay minerals is generally weak due to repulsion from their negatively charged surface [59,60]. However, according to literature data, it is possible for some anions to form strong covalent bonds with the edge sites of clay minerals [61]. Therefore, in order to investigate the sorption processes of various forms of thiophenol, the influence of the contact time of the adsorbate with sepiolite at pH 4, 7 and 9 was investigated.

The saturation of the whole adsorbent mass with the adsorbate depends on the diffusion rate of the molecules adsorbing on it. The achieved state of adsorption equilibrium is expressed by changing the amount of the adsorbed substance over time. Figure 6 shows the effect of contact time with sepiolite on the removal of thiophenol from an aqueous solution with different ionic strengths at pH 4. As shown in Figure 6, the contact time of thiophenol with the clay mineral has a significant impact on the effectiveness of the adsorption process. The ionic strength of the solution has little effect on the sorption kinetics. The greatest differences are observed for a solution with an ionic strength of 0.01. In this case, the sorption process is fastest, most likely due to changes in the electrokinetic properties of the sepiolite. According to Alkan et al. [62], changes in the zeta potential of sepiolite under the influence of NaCl are not significant. However, the presence of monovalent cations in the sepiolite solution usually causes the zeta potential value of the sepiolite to decrease (its surface becomes more negatively charged); then, as the electrolyte concentration increases (above 0.01 M), the value of the zeta potential begins to increase [62].

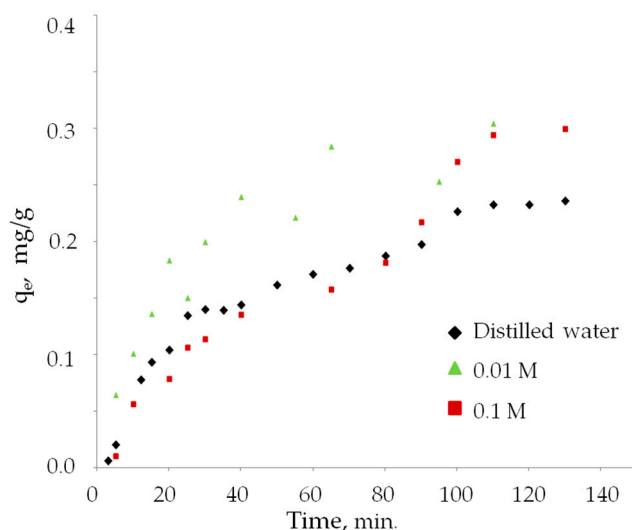


Figure 6. Comparison of the sorption efficiency of thiophenol on sepiolite (pH 4) for three aqueous solutions of thiophenol with different ionic strengths.

As shown in Figure 6, the equilibrium establishment time of the thiophenol adsorption process is relatively long and amounts to 100 min for all solutions. Further contact time did not affect the effectiveness of this process. The adsorption efficiency is relatively low and amounts to approximately 0.23 mg/g for a solution with distilled water (46% of thiophenol removal from 5 mg/L solution was observed). Literature data indicate relatively similar times for establishing sorption equilibrium on sepiolite for dyes from industrial wastewater. The adsorption equilibrium for acid red 57 [63,64] and acid yellow 49 [65] was established within 1 h. Experimental data (Figure 6) indicate that the efficiency of the thiophenol adsorption process is greater for solutions with increased ionic strength: for electrolyte concentrations of 0.01 M and 0.1 M, it is approximately 0.34 and 0.32 mg/g, respectively.

On the other hand, the experimental tests of the sorption process at pH 7 and pH 9 were not successful. During contact of thiophenol with sepiolite for 3 h, no decrease in thiophenol concentration was observed. On the contrary, an increase in thiophenol concentration when in contact with the sepiolite was observed, which indicates the occurrence of a

negative adsorption process. This interesting phenomenon has already been observed, for example, in the case of experiments for aldicarb (2-methyl-2-(methylthio) propionaldehyde O-(methyl-carbamoyl) oxime) on illite and kaolinite clays [66,67].

3.4. The APT Atomic Charges

A thiophenol molecule in alkali/neutral solution has a net electric charge due to its acid–base equilibrium. The charges on individual atoms for three structures, i.e., undissociated thiophenol, the thiophenolate ion and the thiophenolate ion, in the presence of Na⁺ ion (Figure 7), calculated by the DFT/B3LYP/Aug-CC-pVDZ method using the PCM solvation model, are listed in Table 1.

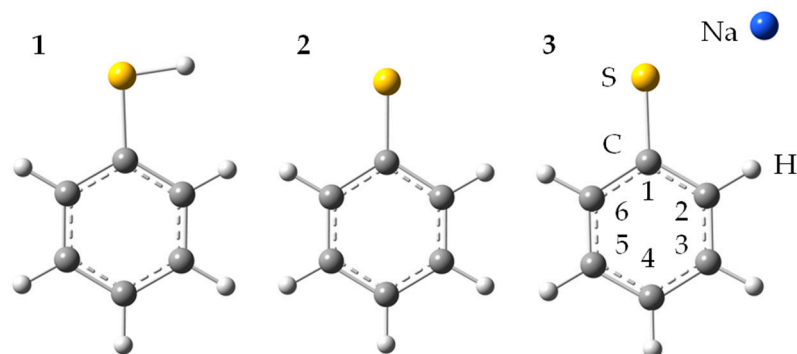


Figure 7. The optimized (DFT/PCM/B3LYP/Aug-CC-pVDZ) structures of pH-dependent forms of thiophenol: (1) thiophenol, (2) thiophenolate ion, (3) sodium thiophenolate.

Table 1. Comparison of APT atomic charges (DFT/PCM/B3LYP/Aug-CC-pVDZ) for different forms of thiophenol (atom numbering in Figure 7) in an aqueous environment.

Atom Number	APT Atomic Charges		
	Thiophenol	Thiophenolate	Sodium Thiophenolate
C1	0.4184	0.5967	0.5844
C2	−0.2027	−0.2761	−0.2684
C3	0.0394	0.1171	0.1087
C4	−0.1388	−0.2831	−0.2598
C5	0.0456	0.1165	0.1032
C6	−0.1906	−0.2753	−0.2654
H(C2)	0.0523	0.0335	0.0376
H(C3)	0.0381	0.0119	0.0154
H(C4)	0.0451	0.02616	0.0287
H(C5)	0.0395	0.0119	0.0149
H(C6)	0.0596	0.0335	0.0265
S	−0.2560	−1.1129	−1.1188
H(S)/Na	0.0501/—	—/—	—/0.9930

According to the data in Table 1, a negative charge appears for all three structures only on the sulfur atom and carbon atoms of the benzene ring in the ortho- and para-positions in relation to the thiol group. Nevertheless, the negative charge of the sulfur atom increases dramatically as the pH increases and the hydrogen atom dissociates. The partial charge on the sulfur atom decreases significantly (from −0.2560 to −1.1129). Additionally, the presence of a sodium atom around the thiolate ion further strengthens this negative charge

(−1.1188, Table 1). Moreover, as the pH increases, the positive charge on all hydrogen atoms of the benzene ring decreases significantly.

Therefore, the results of the analysis of the charge distribution on pH-dependent structures of thiophenol and the fact that the charge on the sepiolite surface is also pH-dependent is consistent with the obtained experimental results. Sepiolite has an isoelectric point at approximately pH 7.1, and at pH 9 the zeta potential value is ca. −20 mV [63,68]. With a decrease in pH, the negative charge of the sepiolite/solution changes and becomes positive (at pH 9, the zeta potential value is ca. −20 mV). In an acidic environment, sorption of thiophenol is possible because thiophenol occurs as a neutral molecule (a small negative charge on the sulfur atom and carbon atoms of the aromatic ring), and the electrokinetic potential at the sepiolite surface is positive. In neutral and alkaline aqueous environments (pH ≥ 7), thiophenolate anions are probably electrostatically pushed from the surface of sepiolite, which has a negative zeta potential in these conditions.

3.5. Adsorption Isotherms

In the literature, due to the multitude of possible sorption mechanisms, various isotherms are used to describe the adsorption process. Adsorption isotherms show the dependence of the amount of adsorbed substance on the concentration of the adsorbate at a given temperature. In this work, the adsorption equilibrium results were fitted to the two most important isotherms: Langmuir and Freundlich [69,70]. The parameters of the isotherm equations were determined using the nonlinear least-squares method using the Levenberg–Marquardt algorithm (minerr function in Mathcad). The results of this fitting are presented in Figure 8 and Table 2.

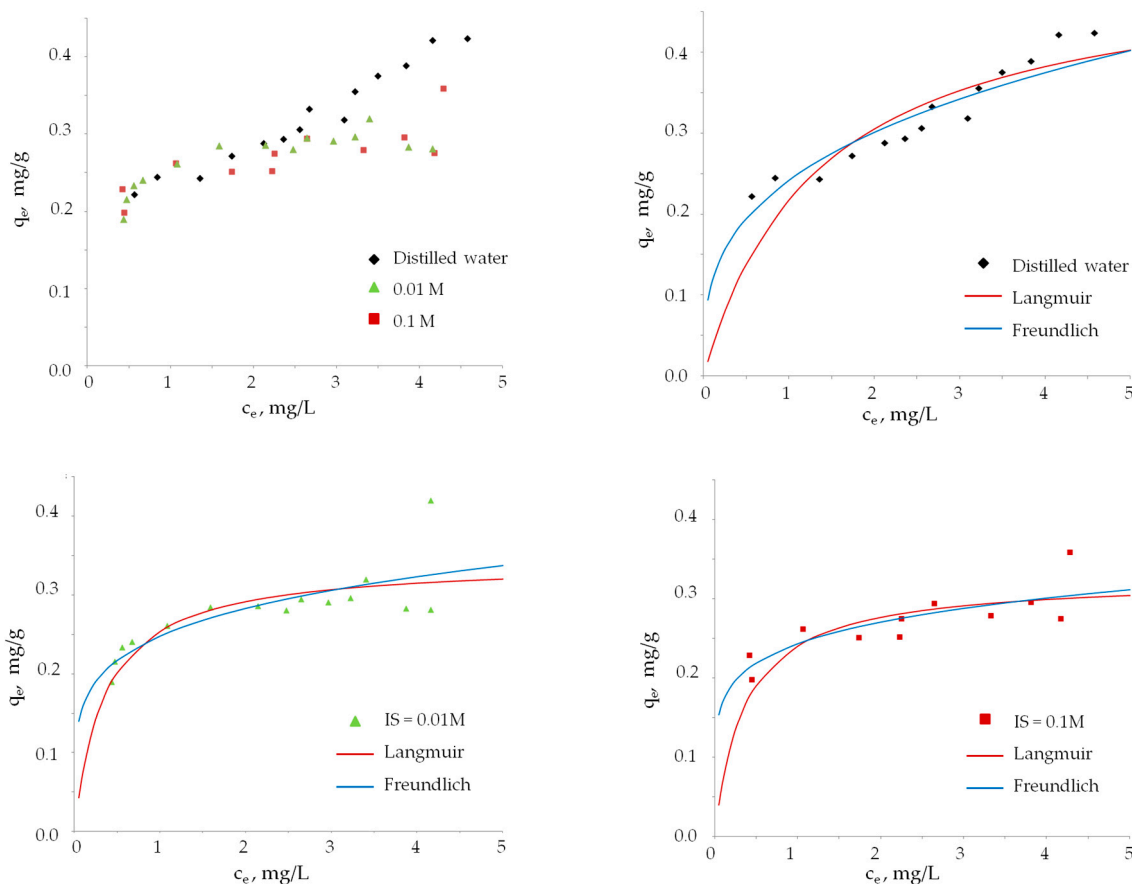


Figure 8. Representation of isotherm models for experimental data of thiophenol adsorption on sepiolite in different ionic strength water solutions at pH 4.

Table 2. The results of fitting the isotherm model (Langmuir and Freundlich) to experimental data for thiophenol adsorption on sepiolite at pH 4.

Solvent	Isotherm Model	Nonlinear Equation	Constants		Quality of Fitting	
			K_L/K_F	$Q_L/(1/n)$	χ^2	RMSE
Distilled water	Langmuir	$q_e = \frac{Q_L \cdot K_L \cdot C_e}{1 + K_L \cdot C_e}$ Plot q_e versus C_e	0.741	0.512	0.065	0.032
0.01 M NaCl			2.855	0.343	0.077	0.040
0.1 M NaCl			2.802	0.326	0.038	0.029
Distilled water	Freundlich	$q_e = K_F \cdot C_e^{1/n}$ Plot q_e versus C_e	0.242	0.316	0.021	0.022
0.01 M NaCl			0.248	0.192	0.069	0.038
0.1 M NaCl			0.243	0.153	0.020	0.023

q_e —equilibrium sorption capacity; K_L —Langmuir constant [L/g]; C_e —equilibrium concentration of sorbate in solution; Q_L —maximum sorption capacity; K_F —Freundlich constant; $1/n$ is the heterogeneity factor; χ^2 —Pearson's Chi-squared test; RMSE—root mean squared error.

The fit of these models is not good, which may indicate a complicated adsorption mechanism. A better approximation for all experimental tests (solutions with different ionic strength) is the Freundlich isotherm model, which indicates the preferred process of physical adsorption of thiophenol on the surface of the tested clay mineral. Values of the $1/n$ parameter ($1/n < 1$) (Table 2) estimated from the Freundlich isotherm equation confirmed that the process of binding thiophenol by sepiolite is physical and this clay mineral has good sorption capacities ($2 < n < 10$) [71]. The K_F parameter values are similar for all three isotherms (0.248–0.242 mg/g), which indicates that the addition of NaCl electrolyte does not significantly affect the sorption properties of sepiolite. The values of the Q_L parameter (maximum sorption capacity, Table 2) determined from the Langmuir equation are greater than (or equal to) the experimental values from kinetic experiments (Figure 6). This may indicate monolayer sorption or a situation in which the monolayer is not completely filled with adsorbate, as is the case with the sorption of thiophenol from a solution prepared from distilled water.

3.6. Infrared Spectroscopy

In Figure 9, the FT-IR spectra of the thiophenol and sepiolite (powder) used as sorbent in this work are shown. The spectrum of sepiolite is identical to the infrared spectrum of this clay mineral from the spectral database (U.S. Geological Survey Minerals Database) and is also consistent with the spectra of sepiolite presented in the literature [72,73]. Additionally, Figure 9 also shows the FT-IR spectrum of the sample of sepiolite after the thiophenol adsorption process at pH 4 (sepiolite + saturated thiophenol solution). The solubility of thiophenol in water is 836 mg/L (25 °C) [74].

Bands originating from the stretching of the –OH groups of sepiolite are observed in the spectral range of 3800–2000 cm^{-1} (Figure 9A). Bands at 3687, 3620, and 3558 cm^{-1} are assigned to vibrations of the –OH groups connected to the magnesium atom, while bands at 3430 and 3260 cm^{-1} are due to zeolitic water in this clay mineral [72]. In this spectral region, the spectra of sepiolite and sepiolite with adsorbed thiophenol do not actually differ. This indicates a lack of binding of thiophenol to charged sites on the sepiolite surface (surface associated with magnesium atoms). In the second range of the spectrum in the infrared range, i.e., 2000–400 cm^{-1} (Figure 9B), small changes are noticeable. They concern bands associated with stretching and deformation vibrations of Si-O groups, which indicates the interaction of thiophenol with the neutral part of the sepiolite surface. As is seen in Figure 9, a decrease in the intensity of the band at 1078 cm^{-1} is observed. The ratio of the intensity of the bands at 1023 and 979 cm^{-1} is changed. Additionally, the band at 474 cm^{-1} , which is assigned to the deformation of Si-O-Si groups is shifted slightly to 470 cm^{-1} . As can be seen in Figure 9, thiophenol is present after the sorption process on sepiolite. This is evidenced by the presence in the spectrum of three bands at 1480, 1442 and 734 cm^{-1} ,

which are the most intense bands in the spectrum of thiophenol [75]. On closer inspection, it can be seen that an additional band is observed at 741 cm^{-1} . These bands are associated with out-of-plane C-H deformations and vibrations of the benzene ring. The appearance of this additional band at 741 cm^{-1} is most likely the result of the physical adsorption of thiophenol on sepiolite. The benzene ring of some thiophenol molecules (which were adsorbed on the mineral surface) interacts with the sepiolite surface and causes a change in the frequency of these vibrations. On the other hand, the bands at 1480 and 1442 cm^{-1} , which are associated with the -CH bending of the benzene ring of thiophenol, are slightly shifted towards lower wavenumbers.

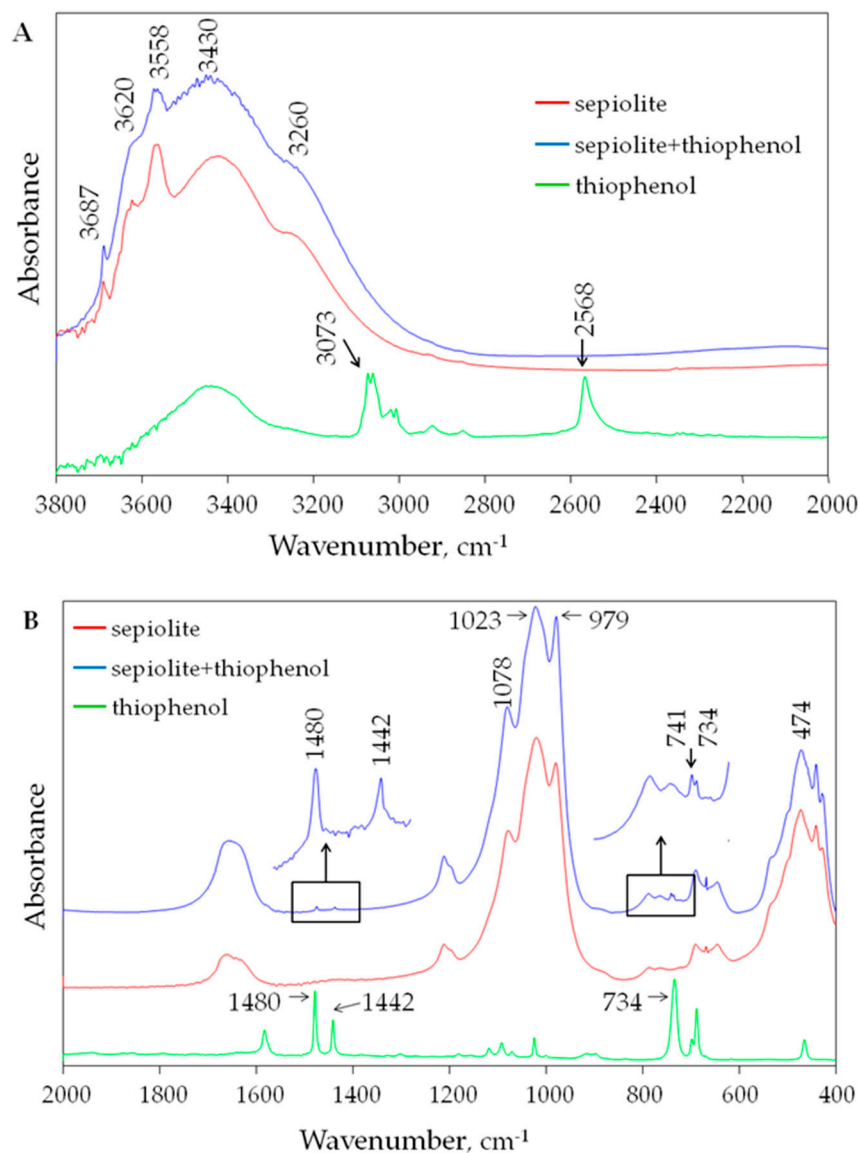


Figure 9. FT-IR spectra of thiophenol, sepiolite (powder) and sepiolite + saturated thiophenol solution in the spectral ranges of $3800\text{--}2000$ (A) and $2000\text{--}400\text{ cm}^{-1}$ (B).

The sorption process of thiophenol on sepiolite using the ATR-FTIR technique was also investigated. This method allows for in situ testing of samples that are aqueous solutions or contain large amounts of water. Figure 10 shows the ATR spectra of sepiolite after 3 h of contact with a saturated thiophenol solution at pH 4, 7 and 9 (after the contact time, the sepiolite was separated from the thiophenol-saturated solution by centrifugation). The result of this study confirms previous observations. As can be seen in Figure 10, thiophenol is adsorbed on the sepiolite surface only in an acidic environment (pH 4). This

is evidenced by the presence in the spectrum of bands originating from thiophenol at 1478 and 1440 cm^{-1} . These bands are not visible in the spectra of the remaining samples (at pH 7 and 9).

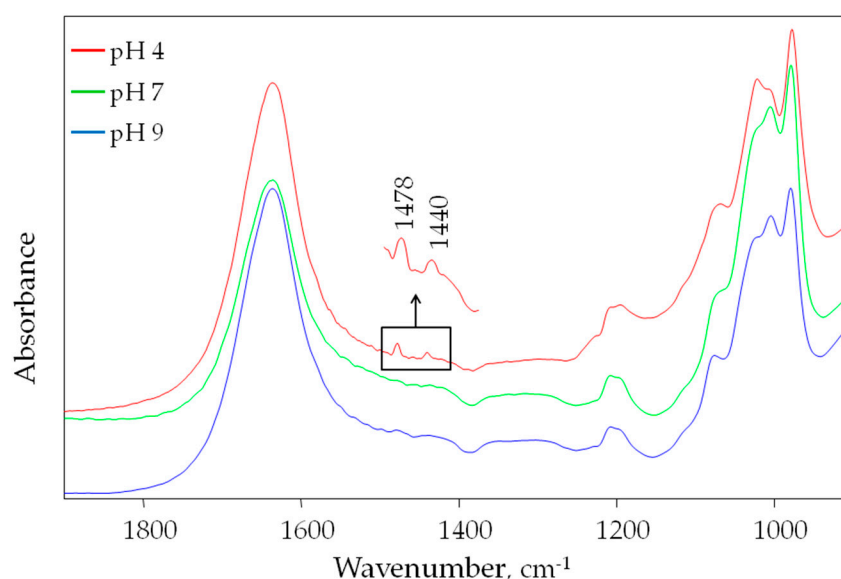


Figure 10. ATR-FTIR spectra of sepiolite after 3 h of contact with a saturated thiophenol solution at pH 4, 7 and 9.

4. Conclusions

Sepiolite is a clay mineral that can be used in water purification systems and as a bottom liner material in solid waste landfills for the retention of organic and inorganic pollutants. In this work, sepiolite was used, for the first time, for removal of toxic thiophenol from water solution. As these are preliminary studies on the use of clay minerals to remove thiophenol, unmodified sepiolite was used in the tests. This did not require processes to modify the mineral surface by conducting reactions requiring the use of additional reagents. Therefore, these studies provide knowledge about sorption processes on natural sepiolite that may occur in the environment. Surface modification of a clay mineral can increase its sorption capacity, which is certainly desirable for industrial use.

Experimental data show that the pH of an aqueous solution is crucial for the adsorption process of thiophenol on sepiolite. Adsorption of thiophenol on sepiolite occurs in an acidic medium (pH 4). The efficiency of this process is low: for the given experimental conditions, it is approximately 0.23–0.34 mg/g (depending on the ionic strength of the solution). At pH 4, the zeta potential of sepiolite is positive, and physical adsorption of neutral thiophenol molecules occurs. This is indicated by a better fit of the Freundlich isotherm than the Langmuir isotherm to the experimental results. Infrared spectroscopy studies show that thiophenol does not interact strongly with the sepiolite surface. The infrared spectra for sepiolite after the thiophenol adsorption process differ slightly from the spectrum of pure sepiolite. Only slight differences in the position and intensity of the bands associated with the vibrations of Si-O bonds are observed, which indicates the interaction of thiophenol with the neutral part of the sepiolite surface.

At pH 7 and 9, adsorption of thiophenol on unmodified sepiolite was not observed. Experiments under these conditions have shown that the concentration of sorbate increases with time in an aqueous solution containing sepiolite, which indicates the occurrence of a phenomenon known as the negative adsorption process. At a higher pH (7 and 9), not only thiophenolate anions ($\text{pK}_a = 6.62$) are formed, but also the zeta potential of sepiolite changes to negative (the isoelectric point of sepiolite is 7.1). No sorption is observed under these conditions. On the contrary, thiophenolate anions are repelled from the sepiolite surface (negative zeta potential) and their concentration in the solution above

the adsorbent surface increases. These observations are consistent with computational data (DFT/PCM/B3LYP/Aug-CC-pVDZ). Calculations of the distribution of charge within a molecule indicate that during the process of thiophenol dissociation (and formation of the thiophenolate anion) a decrease in positive charge is observed throughout the whole molecule. Under such conditions, not only does the thiophenolate anion have a large negative charge on the deprotonated sulfur atom, but also the positive charge on all hydrogen atoms of the benzene ring decreases significantly compared to the neutral thiophenol molecule.

Funding: The project was partly supported by the “Excellence Initiative-Research University” program for AGH University of Krakow. This research was partly funded by AGH University of Krakow, The Faculty of Drilling, Oil and Gas (No. 16.16.190.779).

Data Availability Statement: The data presented in this study are available on request from the author.

Acknowledgments: Academic Computer Centre Cyfronet AGH (Krakow, Poland) is acknowledged for computing time. This research was supported in part by PL-Grid Infrastructure.

Conflicts of Interest: The author declares no conflicts of interest. The funders had no role in the design of the study; in the collection, analyses, or interpretation of data; in the writing of the manuscript, or in the decision to publish the results.

References

1. El-Gendy, N.S.; Speight, J.G. *Handbook of Refinery Desulfurization, Chapter 2 Feedstocks*; CRC Press: Boca Raton, FL, USA, 2015; p. 57.
2. Katasonova, O.N.; Savonina, E.Y.; Maryutina, T.A. Extraction Methods for Removing Sulfur and Its Compounds from Crude Oil and Petroleum Products. *Russ. J. Appl. Chem.* **2021**, *94*, 411–436. [[CrossRef](#)]
3. Shi, Q.; Wu, J. Review on Sulfur Compounds in Petroleum and Its Products: State-of-the-Art and Perspectives. *Energy Fuels* **2021**, *35*, 14445–14461. [[CrossRef](#)]
4. Alzarqani, A.K.; Alduhaidahawi, F.J. The risks of increment of concentrations of sulfur compounds in Iraqi crude oil, gasoline and kerosene. *Int. J. Health Sci.* **2002**, *6*, 283–293.
5. Kondyli, A.; Schrader, W. Study of Crude Oil Fouling from Sulfur-Containing Compounds Using High-Resolution Mass Spectrometry. *Energy Fuels* **2021**, *35*, 13022–13029. [[CrossRef](#)]
6. Kadhum, A.T.; Albayati, T.M. Desulfurization techniques process and future challenges for commercial of crude oil products: Review. *AIP Conf. Proc.* **2022**, *2443*, 030039. [[CrossRef](#)]
7. Javadli, R.; de Klerk, A. Desulfurization of heavy oil. *Appl. Petrochem. Res.* **2012**, *1*, 3–19. [[CrossRef](#)]
8. Saha, B.; Vedachalam, S.; Dalai, A.K. Review on recent advances in adsorptive desulfurization. *Fuel Process. Technol.* **2021**, *214*, 106685. [[CrossRef](#)]
9. Li, J.; Kimb, H.R.; Leeb, H.-M.; Yu, H.C.; Jeon, E.; Lee, S.; Kimb, D.-H. Rapid biodegradation of polyphenylene sulfide plastic beads by *Pseudomonas* sp. *Sci. Total Environ.* **2020**, *720*, 137616. [[CrossRef](#)]
10. Yan, D.-W.; Li, X.-D.; Chen, X.-L.; Cai, S.-J.; Yan, Y.-G.; Ren, H.-H. Breaking the hydrophilic limitation of polyphenylene sulfide through the introduction of bulky polar monomers. *Polymer* **2024**, *291*, 126598. [[CrossRef](#)]
11. Chen, G.; Mohanty, A.K.; Misra, M. Progress in research and applications of Polyphenylene Sulfide blends and composites with carbons. *Compos. Part B Eng.* **2021**, *209*, 108553. [[CrossRef](#)]
12. Ma, J.; Chen, Y.; Xu, Y.; Wei, Y.; Meng, D.; Wang, B.; Zhang, Z. Monitoring thiophenols in both environmental water samples and bio-samples: A method based on a fluorescent probe with broad pH adaptation. *Ecotoxicol. Environ. Saf.* **2022**, *233*, 113340. [[CrossRef](#)]
13. Zin, R.M.; Coquelet, C.; Valtz, A.; Mutalib, M.I.A.; Sabil, K.M.A. New Thermodynamic Correlation for Apparent Henry’s Law Constants, Infinite Dilution Activity Coefficient and Solubility of Mercaptans in Pure Water. *J. Nat. Gas Eng.* **2017**, *2*, 148–170.
14. Hell, T.P.; Lindsay, R.C. Toxicological properties of thio- and alkylphenols causing flavor tainting in fish from the upper Wisconsin River. *J. Environ. Sci. Health Part B* **1989**, *24*, 349–360. [[CrossRef](#)]
15. Serjeant, E.P.; Dempsey, B. *Ionisation Constants of Organic Acids in Aqueous Solution. International Union of Pure and Applied Chemistry (IUPAC); IUPAC Chemical Data Series No. 23*; Pergamon Press, Inc.: New York, NY, USA, 1979; p. 165.
16. Yan, H.; Yue, Y.; Yin, C.; Zhang, Y.; Chao, J.; Huo, F. A water-soluble fluorescent probe for the detection of thiophenols in water samples and in cells imaging. *Spectrochim. Acta Part A Mol. Biomol. Spectrosc.* **2020**, *229*, 117905. [[CrossRef](#)]
17. Zhang, Y.; Hao, Y.; Ma, X.; Chen, S.; Xu, M. A dicyanoisophorone-based highly sensitive and selective near-infrared fluorescent probe for sensing thiophenol in water samples and living cells. *Environ. Pollut.* **2020**, *265*, 114958. [[CrossRef](#)]
18. Choi, M.G.; Cho, M.J.; Ryu, H.; Hong, J.; Chang, S.-K. Fluorescence signaling of thiophenol by hydrolysis of dinitrobenzenesulfonamide of 2-(2-aminophenyl)benzothiazole. *Dye. Pigment.* **2017**, *143*, 123–128. [[CrossRef](#)]

19. Guo, S.-H.; Leng, T.-H.; Wang, K.; Wang, C.-Y.; Shen, Y.-J.; Zhu, W.-H. A colorimetric and turn-on NIR fluorescent probe based on xanthene system for sensitive detection of thiophenol and its application in bioimaging. *Talanta* **2018**, *185*, 359–364. [CrossRef]
20. Khan, N.; Tabasi, Z.A.; Liu, J.; Zhang, B.H.; Zhao, Y. Recent Advances in Functional Materials for Wastewater Treatment: From Materials to Technological Innovations. *J. Mar. Sci. Eng.* **2022**, *10*, 534. [CrossRef]
21. Ewis, D.; Ba-Abbad, M.; Benamor, A.; El-Naas, M. Adsorption of organic water pollutants by clays and clay minerals composites: A comprehensive review. *Appl. Clay Sci.* **2022**, *229*, 106686. [CrossRef]
22. Yu, F.; Bai, X.; Liang, M.; Ma, J. Recent progress on metal-organic framework-derived porous carbon and its composite for pollutant adsorption from liquid phase. *Chem. Eng. J.* **2021**, *405*, 126960. [CrossRef]
23. Lazaratou, C.V.; Vayenas, D.V.; Papoulis, D. The role of clays, clay minerals and clay-based materials for nitrate removal from water systems: A review. *Appl. Clay Sci.* **2020**, *185*, 105377. [CrossRef]
24. Li, T.; Cai, G.; Wang, C.; Liang, K.; Ma, S.; Luo, W. Quantifying clay mineral sources in marine sediments by using end-member mixing analysis. *Geo-Mar. Lett.* **2021**, *41*, 6. [CrossRef]
25. Chaerun, S.K.; Tazaki, K. How kaolinite plays an essential role in remediating oil-polluted seawater. *Clay Miner.* **2005**, *40*, 481–491. [CrossRef]
26. Nagy, B.; Bradley, W.F. The structural scheme of sepiolite. *Am. Mineral.* **1955**, *40*, 885–892. [CrossRef]
27. Available online: <https://www.handbookofmineralogy.org/pdfs/sepiolite.pdf> (accessed on 27 April 2024).
28. Brauner, K.; Preisinger, A. Struktur und Entstehung des Sepioliths. *Tschermaks Mineral. Petrogr. Mitteilungen* **1956**, *6*, 120–140. [CrossRef]
29. Brindley, G.W. X-ray and electron diffraction data for sepiolite. *Am. Mineral.* **1959**, *44*, 495–500.
30. Post, J.E.; Bish, D.L.; Heaney, P.J. Synchrotron powder X-ray diffraction study of the structure and dehydration behavior of sepiolite. *Am. Mineral.* **2007**, *92*, 91–97. [CrossRef]
31. Giustetto, R.; Levy, D.; Wahyudi, O.; Ricchiardi, G.; Vitillo, J.G. Crystal structure refinement of a sepiolite/indigo Maya Blue pigment using molecular modelling and synchrotron diffraction. *Eur. J. Mineral.* **2011**, *23*, 449–466. [CrossRef]
32. Suarez, M.; Garcia-Romero, E. Variability of the surface properties of sepiolite. *Appl. Clay Sci.* **2012**, *67–68*, 72–82. [CrossRef]
33. Nishimura, Y.; Hori, Y.; Takahashi, H. Structural change and adsorption character of sepiolite by heat treatment. *J. Gay Sci. Soc. Jpn.* **1972**, *12*, 102–108.
34. Shuali, O.; Nir, S.; Rytwo, G. Adsorption of surfactants, dyes and cationic herbicides on sepiolite and palygorskite: Modifications, applications and modelling, Ch 15. In *Developments in Palygorskite-Sepiolite Research, A New Look at These Materials*; Galan, E., Singer, A., Eds.; Elsevier: Amsterdam, The Netherlands, 2011.
35. Rytwo, G.; Nir, S.; Margulies, L.; Casal, B.; Merino, J.; Ruiz-Hitzky, E.; Serratos, J.M. Adsorption of Monovalent Organic Cations on Sepiolite: Experimental Results and Model Calculations. *Clays Clay Miner.* **1998**, *46*, 340–348. [CrossRef]
36. Wu, J.; Wang, Y.; Wu, Z.; Gao, Y.; Li, X. Adsorption properties and mechanism of sepiolite modified by anionic and cationic surfactants on oxytetracycline from aqueous solutions. *Sci. Total Environ.* **2020**, *708*, 134409. [CrossRef]
37. Largo, F.; Haounati, R.; Ouachtak, H.; Hafid, N.; Jada, A.; Addi, A.A. Design of organically modified sepiolite and its use as adsorbent for hazardous Malachite Green dye removal from water. *Water Air Soil Pollut.* **2023**, *234*, 183. [CrossRef]
38. Gao, S.; Wang, D.; Huang, Z.; Su, C.; Chen, M.; Lin, X. Recyclable NiO/sepiolite as adsorbent to remove organic dye and its regeneration. *Sci. Rep.* **2022**, *12*, 2895. [CrossRef]
39. Yu, J.; He, W.; Liu, B. Adsorption of Acid Orange II with Two Step Modified Sepiolite: Optimization, Adsorption Performance, Kinetics, Thermodynamics and Regeneration. *Int. J. Environ. Res. Public Health* **2020**, *17*, 1732. [CrossRef]
40. De Wild, P.J. Method for Desulphurisation of Natural Gas. Patent US20060058565A1, 16 March 2006.
41. Zadaka-Amir, D.; Bleiman, N.; Mishaal, Y.G. Sepiolite as an effective natural porous adsorbent for surface oil-spill. *Microporous Mesoporous Mater.* **2013**, *169*, 153–159. [CrossRef]
42. Wang, Z.; Liao, L.; Hursthouse, A.; Song, N.; Ren, B. Sepiolite-Based Adsorbents for the Removal of Potentially Toxic Elements from Water: A Strategic Review for the Case of Environmental Contamination in Hunan, China. *Int. J. Environ. Res. Public Health* **2018**, *15*, 1653. [CrossRef]
43. Guney, Y.; Cetin, B.; Aydilek, A.H.; Tanyu, B.F.; Koparal, S. Utilization of sepiolite materials as a bottom liner material in solid waste landfills. *Waste Manag.* **2014**, *34*, 112–124. [CrossRef]
44. Guney, Y.; Koparal, S.; Aydilek, A.H. Sepiolite as an Alternative Liner Material in Municipal Solid Waste Landfills. *J. Geotech. Geoenviron. Eng.* **2008**, *134*, 1166–1180. [CrossRef]
45. Khan, S.; Ajmal, S.; Hussain, T.; Ur Rahman, M. Clay-based materials for enhanced water treatment: Adsorption mechanisms, challenges, and future directions. *J. Umm Al-Qura Univ. Appl. Sci.* **2023**. [CrossRef]
46. Bandura, L.; Wozniak, A.; Kołodziejka, D.; Franus, W. Application of Mineral Sorbents for Removal of Petroleum Substances: A Review. *Minerals* **2017**, *7*, 37. [CrossRef]
47. Zhao, J.; Zhu, Z.-W.; Zhao, D.-X.; Yang, Z.-Z. Atomic charges in molecules defined by molecular real space partition into atomic subspace. *Phys. Chem. Chem. Phys.* **2023**, *25*, 9020–9030. [CrossRef]
48. Foresman, J.B.; Frisch, A. *Exploring Chemistry with Electronic Structure Methods*, 2nd ed.; Gaussian Inc.: Pittsburgh, PA, USA, 1996.
49. Cioslowski, J. A new population analysis based on atomic polar tensors. *J. Am. Chem. Soc.* **1989**, *111*, 8333–8336. [CrossRef]
50. Milani, A.; Castiglioni, C. Atomic charges from atomic polar tensors: A comparison of methods. *J. Mol. Struct. THEOCHEM* **2010**, *955*, 158–164. [CrossRef]

51. Frisch, M.J.; Trucks, G.W.; Schlegel, H.B.; Scuseria, G.E.; Robb, M.A.; Cheeseman, J.R.; Scalmani, G.; Barone, V.; Petersson, G.A.; Nakatsuji, H.; et al. *Gaussian 16, Revision C.01*; Gaussian, Inc.: Wallingford, CT, USA, 2016.
52. Becke, A.D. Density-functional exchange-energy approximation with correct asymptotic behavior. *Phys. Rev. A* **1988**, *38*, 3098. [[CrossRef](#)]
53. Lee, C.; Yang, W.; Parr, R.G. Development of the Colle-Salvetti correlation-energy formula into a functional of the electron density. *Phys. Rev. B* **1988**, *37*, 785. [[CrossRef](#)]
54. Dunning, T.H. Gaussian basis sets for use in correlated molecular calculations. I. The atoms boron through neon and hydrogen. *J. Chem. Phys.* **1989**, *90*, 1007–1023. [[CrossRef](#)]
55. Yebra-Rodriguez, A.; Martin-Ramos, J.; Del Rey, F.; Viseras, C.; Lopez-Galindo, A. Effect of acid treatment on the structure of sepiolite. *Clay Miner.* **2003**, *38*, 353–360. [[CrossRef](#)]
56. Pouly, F.; Touraud, E.; Buisson, J.-F.; Thomas, O. An alternative method for the measurement of mineral sulphide in wastewater. *Talanta* **1999**, *50*, 737–742. [[CrossRef](#)]
57. Roig, B.; Chalmin, E.; Touraud, E.; Thomas, O. Spectroscopic study of dissolved organic sulfur (DOS): A case study of mercaptans. *Talanta* **2002**, *56*, 585–590. [[CrossRef](#)]
58. Borisovera, M.; Davisb, J.A. Chapter 2—Adsorption of Inorganic and Organic Solutes by Clay Minerals. In *Natural and Engineered Clay Barriers*; Tournassat, C., Steefel, C.I., Bourg, I.C., Bergaya, F., Eds.; Book Series: Developments in Clay, Science; Elsevier: Amsterdam, The Netherlands, 2015; Volume 6, pp. 33–70.
59. Jan, Y.-L.; Tsai, S.-C.; Wei, Y.-Y.; Tung, N.-C.; Wei, C.-C.; Hsu, C.-N. Coupled mechanics, hydraulics and sorption properties of mixtures to evaluate buffer/backfill materials. *Phys. Chem. Earth* **2007**, *32*, 789–794. [[CrossRef](#)]
60. Vinsova, H.; Konirova, R.; Koudelkova, M.; Jedinakova-Krizova, V. Sorption of technetium and rhenium on natural sorbents under aerobic conditions. *J. Radioanal. Nucl. Chem.* **2004**, *261*, 407–413. [[CrossRef](#)]
61. Goldberg, S. Competitive adsorption of arsenate and arsenite on oxides and clays. *Soil Sci. Soc. Am. J.* **2002**, *66*, 413–421. [[CrossRef](#)]
62. Alkan, M.; Demirbaş, Ö.; Dogan, M. Electrokinetic properties of sepiolite suspensions in different electrolyte media. *J. Colloid Interface Sci.* **2005**, *281*, 240–248. [[CrossRef](#)]
63. Alkan, M.; Demirbaş, Ö.; Çelikçapa, S.; Doğan, M. Sorption of acid red 57 from aqueous solution onto sepiolite. *J. Hazard. Mater.* **2004**, *116*, 135–145. [[CrossRef](#)]
64. Majdan, M.; Sabah, E.; Bujacka, M. Właściwości adsorpcyjne sepiolitu (Adsorption properties of sepiolite). *Przemysł Chem.* **2008**, *87*, 1022–1028.
65. Alkan, M.; Demirbaş, Ö.; Dogan, M. Removal of acid yellow 49 from aqueous solution by adsorption. *Fresenius Environ. Bull.* **2004**, *13*, 1112–1121.
66. Lambert, J.-F. Organic pollutant adsorption on clay minerals, Developments in Clay Science. *Surf. Interface Chem. Clay Miner.* **2018**, *9*, 195–253.
67. Supak, J.R.; Swoboda, A.R.; Dixon, J.B. Adsorption of Aldicarb by Clays and Soil Organo-Clay Complexes. *Soil Sci. Soc. Am. J.* **1977**, *42*, 244–248. [[CrossRef](#)]
68. Alkan, M.; Tekin, G.; Namli, H. FTIR and zeta potential measurements of sepiolite treated with some organosilanes. *Microporous Mesoporous Mater.* **2005**, *84*, 75–83. [[CrossRef](#)]
69. Shahbeig, H.; Bagheri, N.; Ghorbanian, S.A.; Hallajisani, A.; Poorkarimi, S. A new adsorption isotherm model of aqueous solutions on granular activated carbon. *World J. Model. Simul.* **2013**, *9*, 243–254.
70. Redlich, O.; Peterson, D.L. A useful adsorption isotherm. *J. Phys. Chem.* **1959**, *63*, 1024–1026. [[CrossRef](#)]
71. Brdar, M.; Sciban, M.; Takaci, A.; Dosenovic, T. Comparison of two and three parameters adsorption isotherm for Cr(VI) onto Kraft lignin. *Chem. Eng. J.* **2012**, *183*, 108–111. [[CrossRef](#)]
72. Wałczyk, A.; Michalik, A.; Napruszewska, B.D.; Joanna, K.C.; Karcz, R.; Duraczyńska, D.; Socha, R.; Olejniczak, Z.; Gaweł, A.; Agnieszka, K.; et al. New insight into the phase transformation of sepiolite upon alkali activation: Impact on composition, structure, texture, and catalytic/sorptive properties. *Appl. Clay Sci.* **2020**, *195*, 105740. [[CrossRef](#)]
73. Madejová, J.; Gates, W.P.; Petit, S. Chapter 5—IR Spectra of Clay Minerals. In *Infrared and Raman Spectroscopies of Clay Minerals*; Gates, W.P., Klopogge, J.T., Madejová, J., Bergaya, F., Eds.; Book Series: Developments in Clay, Science; Elsevier: Amsterdam, The Netherlands, 2017; Volume 8, pp. 107–149.
74. Hine, J.; Mookerjee, P.K. The intrinsic hydrophilic character of organic compounds. Correlations in terms of structural contributions. *J. Org. Chem.* **1975**, *40*, 292–298. [[CrossRef](#)]
75. Giresse, C.; Tetsassi, F.; Liégeois, V. Analyzing the Vibrational Signatures of Thiophenol Adsorbed on Small Gold Clusters by DFT Calculations. *ChemPhysChem* **2013**, *14*, 1633–1645.

Disclaimer/Publisher’s Note: The statements, opinions and data contained in all publications are solely those of the individual author(s) and contributor(s) and not of MDPI and/or the editor(s). MDPI and/or the editor(s) disclaim responsibility for any injury to people or property resulting from any ideas, methods, instructions or products referred to in the content.